

Historical behaviour of Dome C and Talos Dome (East Antarctica) as investigated by snow accumulation and ice velocity measurements

Stefano Urbini^a, Massimo Frezzotti^{b,*}, Stefano Gandolfi^c, Christian Vincent^d,
Claudio Scarchilli^b, Luca Vittuari^c, Michel Fily^d

^a *Istituto Nazionale di Geofisica e Vulcanologia, Via di Vigna Murata 605, 00143 Roma, Italy*

^b *Ente per le Nuove Tecnologie, l'Energia e l'Ambiente, Via Anguillarese, 301, 00123 Roma, Italy*

^c *Dipartimento di Ingegneria delle Strutture, dei Trasporti, delle Acque, del Rilevamento, del Territorio, V.le Risorgimento 2, 40086 Bologna, Italy*

^d *Laboratoire de Glaciologie et Géophysique de l'Environnement, CNRS-UJF, 54 rue Molière, Grenoble, France*

Received 9 March 2007; accepted 14 August 2007

Available online 29 August 2007

Abstract

Ice divide–dome behaviour is used for ice sheet mass balance studies and interpretation of ice core records. In order to characterize the historical behaviour (last 400 yr) of Dome C and Talos Dome (East Antarctica), ice velocities have been measured since 1996 using a GPS system, and the palaeo-spatial variability of snow accumulation has been surveyed using snow radar and firn cores. The snow accumulation distribution of both domes indicates distributions of accumulation that are non-symmetrical in relation to dome morphology. Changes in spatial distributions have been observed over the last few centuries, with a decrease in snow accumulation gradient along the wind direction at Talos Dome and a counter-clockwise rotation of accumulation distribution in the northern part of Dome C. Observations at Dome C reveal a significant increase in accumulation since the 1950s, which could correlate to altered snow accumulation patterns due to changes in snowfall trajectory. Snow accumulation mechanisms are different at the two domes: a wind-driven snow accumulation process operates at Talos Dome, whereas snowfall trajectory direction is the main factor at Dome C. Repeated GPS measurements made at Talos Dome have highlighted changes in ice velocity, with a deceleration in the NE portion, acceleration in the SW portion and migration of dome summit, which are apparently correlated with changes in accumulation distribution. The observed behaviour in accumulation and velocity indicates that even the most remote areas of East Antarctica have changed from a decadal to secular scale.

© 2007 Elsevier B.V. All rights reserved.

Keywords: geophysical survey; ice divide; snow accumulation; Talos Dome; Dome C; East Antarctica

1. Introduction

One of the most extreme environments on the Earth's surface is the ice divide extending from Dronning Maud Land (DML) to Talos Dome (TD) in inner East Antarctica (Fig. 1). Due to extremely difficult field conditions in the

inner part of East Antarctica, the accumulation pattern and evolution of the dome–ice divide is poorly known. The Earth's oldest ice cores were obtained along or near this ice divide (EPICA DML, Dome Fuji, EPICA Dome C, Vostok). Dome C (DC), Antarctica's fourth highest dome (3233 m), is about 1200 km from the Southern Ocean. The French–Italian Concordia Station (123°20'52"E, 75°06'04"S), where the EPICA (European Project for Ice Coring in Antarctica) drilling site is located, is about 1.4 km west

* Corresponding author. Tel.: +39 06 30483271; fax: +39 06 30486678.
E-mail address: frezzotti@casaccia.enea.it (M. Frezzotti).

of the DC surface summit. TD is an ice dome on the edge of the East Antarctic plateau (159°04'21"E, 72°47'17"S; 2318 m), about 1100 km East of DC (Fig. 1) and about 280 km from the Southern Ocean and Ross Sea.

In December 2004 a 3270 m deep ice core was recovered at DC within the framework of EPICA. This core provides the oldest existing ice climate record, extending to 740,000 yr before the present (EPICA community, 2004). In 2004, a new ice coring project, TALDICE (Talos Dome Ice Core Project), was started at TD with the aim of recovering 1550 m of ice that spans the last 120,000 yr (Frezzotti et al., 2004a). Ice divide–dome migration cannot be directly detected. However, the stability of the dome and position of the ice divide must be known in order to accurately interpret ice core records and to complete ice sheet mass balance studies. Models of depth–age relations for deep ice cores are sensitive to migration of the dome position (Anandakrishnan et al., 1994). Ice divide migration is also important in determining the input parameter of large Antarctic drainage basins. The behaviour of an ice divide is driven by its accumulation rate history and spatial pattern and conditions at ice sheet boundaries (e.g. Hindmarsh, 1996; Nereson et al., 1998; Frezzotti et al., 2004a). Indeed, surface elevations at DC, Vostok and Dome Fuji have varied by up to 100–150 m between glacial and interglacial periods due to changes in accumulation (Ritz et al., 2001).

The low slope (less than 1 dm per km) of the East Antarctic domes and their surface morphology at meter scale (e.g., sastrugi) makes it very difficult to determine the summit point of the dome and its migration over time.

The objective of this paper is to provide information on the historical behaviour of DC and TD using snow accumulation distribution during the last 400 yr as revealed by detailed snow accumulation, radar derived isochrones and ice dynamic changes based on ice velocity measurements made over the last 10 yr.

These data should be very useful in the future for determining changes in mass balance and thickness in these areas and detecting the possible impact of climate change to the ice core. DC and TD are also interesting sites for comparisons with satellite observations and numerical modelling.

2. Materials and methods

Internal layers of strong radar that are reflectively observed with Ground Penetrating Radar (GPR) are isochronous, and surveys along continuous profiles provide detailed information on spatial variability in snow accumulation (e.g., Richardson et al., 1997;

Vaughan et al., 1999; Frezzotti et al., 2002; Eisen et al., 2004; Spikes et al., 2004; Frezzotti et al., 2005). For the purposes of this study, sixteen shallow snow–firn cores were drilled in the DC area and six in the TD area (Vincent and Pourchet, 2000; Frezzotti et al., 2004a, 2005, 2007). All core sites were linked through GPR and GPS (Global Positioning System) surveys in order to gain detailed insight into the spatial variability of snow accumulation. Strain networks established in the DC and TD areas have been surveyed (using static GPS and DORIS measurements) since 1993 (Frezzotti et al., 2004a; Vittuari et al., 2004).

2.1. Snow accumulation and isochrones

A total of 800 km of GPR and kinematic GPS surveys (500 km at DC, 300 km at TD) were carried out within a 25 km radius of the domes. GPS surveys were integrated with previous surveys to create a detailed topographic map (Cefalo et al., 1996; Capra et al., 2000; Frezzotti et al., 2004a). The accuracy of the GPS elevation profile is about 10 cm; the interpolation process reduces accuracy to about 20 cm in the maps. Due to a very low slope in the summit area, surface morphology at meter scale (e.g., sastrugi, barchans etc.) and instrumental error, it is very difficult to define the precise position of the dome summit. Therefore, we identified the dome summit as the area inside the highest contour line.

GPR data acquisition was performed using a GSSI Sir10B unit equipped with two monostatic antennas with a central frequency of 400 and 900 MHz at DC and one monostatic antenna with a central frequency of 200 MHz at TD. The traces were recorded at about one scan per meter in a 150 ns time window for the 900 MHz antenna (14–15 m), a 350 ns time window for the 400 MHz antenna (33–35 m investigation depth) and a 750 ns time window for the 200 MHz antenna (60–70 m). A rate of 4 scans s⁻¹ and 1024 samples per trace were chosen for antennas. Post-processing of GPR data involved gain ranging, low and high bandpass filtering and trace stacking. The recorded two-way travel times (TWT) were converted to depths following the density–depth information-based methodology outlined in Frezzotti et al. (2002). Density information was obtained from 16 firn cores (from 6 to 50 m deep) and 1 trench (3 m deep) at DC and 3 firn/ice cores (from 26 to 89 m deep) and 2 trenches (2.5 m deep) at TD. Density profile analysis revealed no detectable geographical variation in density or compaction within the dome areas. All density data were therefore fitted with a second-order polynomial function for each dome area; this yielded a correlation coefficient (R^2) of more than 0.9 for both measured and computed

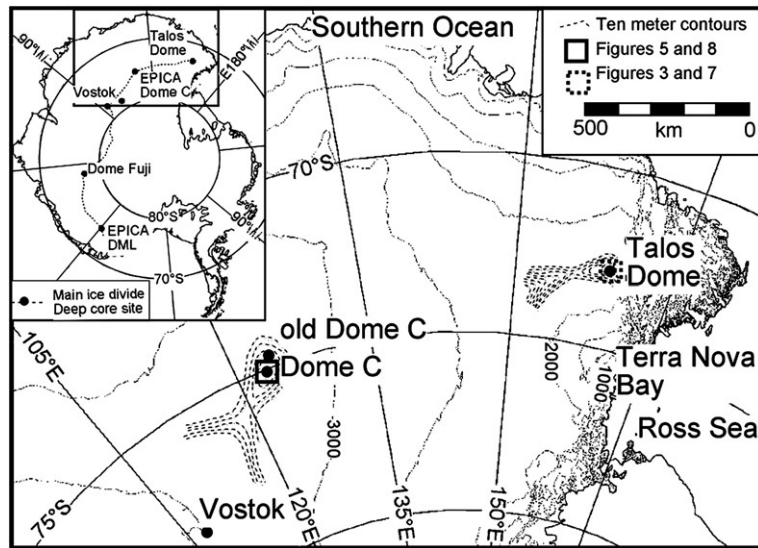


Fig. 1. Schematic map with 500 m contour intervals; the 10 m contours in the Dome C and Talos Dome area are derived from a Digital Elevation Model provided by Brisset and Rémy (1996).

densities. The integration of density measurements yielded cumulative mass as a density–depth function along each radar profile. Given the small differences in density at isochrone depths (max difference in depth 1 m), the snow compaction rate difference between sites is

negligible for calculation purposes. Layer thinning due to vertical strain can be also considered to be negligible ($3 \times 10^{-5} \text{ yr}^{-1}$).

Six continuous internal layers were tracked along all profiles at DC (L1 and L2 with the 900 MHz antenna

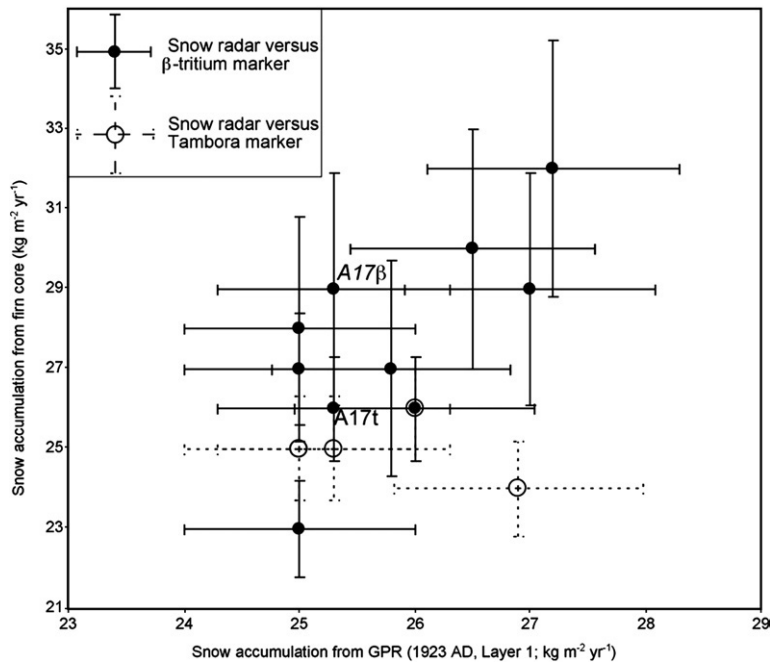


Fig. 2. Comparison of snow accumulation from snow radar (L1 calibrated using the depth–age function at EPICA) versus snow accumulation derived from firn core analysis (A17β: Beta marker and A17t: tritium marker) within a 25 km radius of Dome C.

Table 1

Position (2002 AD) of the stakes at Talos Dome, annual movement (velocity, direction) and acceleration–deceleration (from 1996–98 to 2002–05 AD)

Station ID	Lat. S	Long. E	1996–1998 (δ yr 2.12)	1998–2002 (δ yr 3.03)	2002–2005 (δ yr 3.04)	Acceleration (mm yr ⁻²)
TD01	72°48′03″	159°05′46″				-2±3
Dir. (°)			327	171	177	
Vel. (mm yr ⁻¹)			56±13	40±9	44±9	
TD02	72°43′41″	159°06′45″				-4±3
Dir. (°)			29	15	14	
Vel. (mm yr ⁻¹)			114±13	112±9	90±9	
TD03	72°44′55″	159°16′19″				-5±3
Dir. (°)			76	73	78	
Vel. (mm yr ⁻¹)			343±13	324±9	314±9	
TD04	72°48′04″	159°20′28″				-5±3
Dir. (°)			82	80	82	
Vel. (mm yr ⁻¹)			336±13	302±9	307±9	
TD05	72°51′01″	159°16′21″				-3±3
Dir. (°)			122	125	124	
Vel. (mm yr ⁻¹)			161±13	131±9	143±9	
TD06	72°52′19″	159°05′58″				1±3
Dir. (°)			185	189	191	
Vel. (mm yr ⁻¹)			293±13	301±9	300±9	
TD07	72°51′03″	158°55′38″				3±3
Dir. (°)			202	206	206	
Vel. (mm yr ⁻¹)			270±13	288±9	290±9	
TD08	72°47′59″	158°51′24″				4±3
Dir. (°)			233	246	242	
Vel. (mm yr ⁻¹)			104±13	124±9	125±9	
TD09	72°44′56″	158°55′44″				4±3
Dir. (°)			318	310	305	
Vel. (mm yr ⁻¹)			137±13	156±9	158±9	

and L3, L4, L5 and L6 with the 400 MHz antenna) and four along profiles at TD (L3, L4, L5 and L6 with the 200 MHz antenna). Depth uncertainty in GPR data was estimated to be about ± 14 cm for data acquired with the 200 MHz antenna (TD), ± 6 cm for data acquired with the 400 MHz antenna and ± 3 cm for the 900 MHz antenna (DC). Layer depths measured at intersecting points were in good agreement (± 25 cm for 200 MHz, ± 15 cm for 400 MHz and ± 10 cm for 900 MHz). Layer data were mapped using Kriging interpolation (linear semivariogram, nugget equal to 0.003) to draw snow accumulation and palaeo-maps.

Stratigraphic dating of EPICA (Udisti et al., 2000; Castellano et al., 2005), through non-sea-salt (nss) SO₄²⁻ spikes from the past volcanic events (Pinatubo 1992 AD, Agung 1964 AD, Krakatua 1887 AD, Tambora 1816 AD, Jorull-Taal 1758 AD, Serua 1696 AD, Huaynaputina 1601 AD, Kuwae 1460 AD), was used to establish the depth–age function of the GPR isochrones at DC. Analogously at TD, the age of GPR isochrones was estimated using stratigraphic dating of TD core (Stenni et al., 2002) through seasonal variations in nssSO₄²⁻ concentrations coupled with the identification of tritium

marker levels (1965–66 AD) and nssSO₄²⁻ spikes from past volcanic events (Pinatubo 1992 AD, Agung 1964 AD, Rabaul 1938 AD, Krakatua 1887 AD, Consequina 1837 AD, Tambora 1816 AD, Serua 1696 AD, Huaynaputina 1601 AD, Kuwae 1460 AD).

According to the defined depth–age function, the depth of layers L1 (5.7 m) and L2 (9.1 m) at the EPICA site was dated to 1921 ± 3 and 1869 ± 3 AD, respectively; layer L5 (16.4 m) was dated to 1739 ± 7 AD, whereas the deepest layer L6 (23.2 m) was dated to 1602 ± 9 AD. Previously, Frezzotti et al. (2004a) used the same methodology to establish a depth–age function at TD core sites; S1 (14.8 m) dates to 1920 ± 2 AD, S2 (26.7 m) to 1835 ± 2 AD, S3 (49.3 m) to 1635 ± 5 AD and the deepest traceable S4 (61.2 m) to 1525 ± 5 AD.

The snow accumulation rate of 16 firn cores within a 25 km radius of DC (Vincent and Pourchet, 2000; Frezzotti et al., 2005) was determined for the last 50 yr using β and tritium peaks from 1965 to 1966 AD atmospheric thermonuclear bomb tests and for the past two centuries using the Tambora marker (1816 AD). The experimental error ($\pm \sigma_e$) in calculated snow accumulation rates using firn core is estimated to be less than 10% for β -

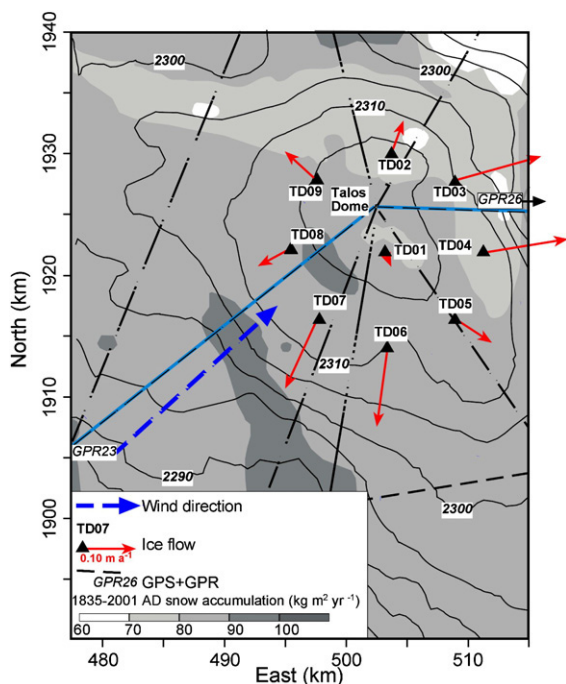


Fig. 3. Talos Dome snow accumulation map ($\text{kg m}^{-2} \text{yr}^{-1}$) based on snow radar data (S2: 1835–2001 AD). Contour lines of surface topography have a 5 m interval. Snow radar profiles (dotted line), vector ice velocity (red arrow) and prevalent wind direction (blue arrow) are shown. The cyan line indicates the elevation and snow radar profile of Fig. 4.

radioactivity (1965–2000 AD) and less than 5% for both the tritium period (1966–1998 AD) and the period since Tambora (1816–1998 AD; Fig. 2).

2.2. Velocity measurements

Surface strain networks consisted of 9 stakes at TD and 37 stakes at DC. Stakes were placed 8 km away from the centre of TD and 3, 6, 12.5 and 25 km from the centre of DC. GPS measurements of the networks were completed 4 times at TD (Table 1) and 2 times at DC. Reference poles (located close to the dome summits) were positioned on the basis of static GPS measurements; the Terra Nova Bay permanent GPS station was the base station for TD, while DORIS was the base station for DC. Process details are reported elsewhere (Frezzotti et al., 2004a; Vittuari et al., 2004). Here, we present the results of 4 repeated measurements performed at TD (Table 1) between the end of 1996 and the beginning of 2005 (Nov 1996; Dec 1998; Jan 2002; Jan 2005). The estimated uncertainty between two GPS positions at TD is ~ 28 mm, with an uncertainty of less than 10 mm yr^{-1} for 1998–2002 measurements and $\sim 14 \text{ mm yr}^{-1}$ for 1996–98 and 2002–2005 measure-

ments; the uncertainty in acceleration is estimated to be $\sim 2.5 \text{ mm yr}^{-2}$ for measurements taken 5.6 yr apart.

3. Results and discussion

3.1. Spatial and temporal accumulation distribution

3.1.1. Talos Dome

Based on the depth distribution of snow layers, Frezzotti et al. (2004a, 2007) found that accumulation decreases downwind of TD (N–NE) and is higher in the SSW sector (Fig. 3). TD surface contour lines are elliptical and elongated in a NW–SE direction; the NW and NE slopes are steeper. The elongation direction of the dome is perpendicular to the prevalent wind direction and parallel to both the outcropping Outback Nunataks (50 km North to TD) and the sharp NW–SE ridge in the bedrock. At TD, wind blows uphill from the SW with a gradient of $1\text{--}2 \text{ m km}^{-1}$ for a distance of 100 km. As pointed out by Frezzotti et al. (2007), the higher accumulation in the SSW sector is correlated with reduced wind-driven sublimation in this area, which is due to the positive slope gradient that reduces wind velocities. The lower accumulation in the downwind sector is ascribable to an increase in wind-driven sublimation, which was determined by the increase in the surface slope toward the Southern Ocean (Figs. 1 and 3).

Analysis of the palaeo-accumulation map (Figs. 4 and 5) shows the spatial and temporal variability of accumulation over the last four centuries. During the period 1835–1920 AD, the accumulation value is significantly lower compared to the previous (1635–1835 AD) and subsequent (1920–2001 AD) dates in the SW portion, whereas accumulation in the NE sector is more constant across periods. The decrease in the SW part significantly reduces the accumulation gradient along the wind direction (Fig. 4) during the 1835–1920 AD period. An analysis of summit isochrone positions in the past reveals a possible SE migration of about 3.5 m yr^{-1} since the deposition of layer S4 (1526 AD). The δD recorded for the TD core shows a cooler condition and a decrease in snow accumulation during the Little Ice Age (LIA), followed by an increasing trend in δD up to the 1920s–1930s and then negative values during the periods 1930s–1996 AD. Cooler atmospheric temperature conditions in the TD area during the LIA may have increased the persistence of katabatic winds (Stenni et al., 2002). Precipitation reflects large (synoptic) scale phenomena related to circulation on a global scale and is homogenous on a large scale (hundreds of km^2), but wind-driven sublimation phenomena determined by the surface slope along

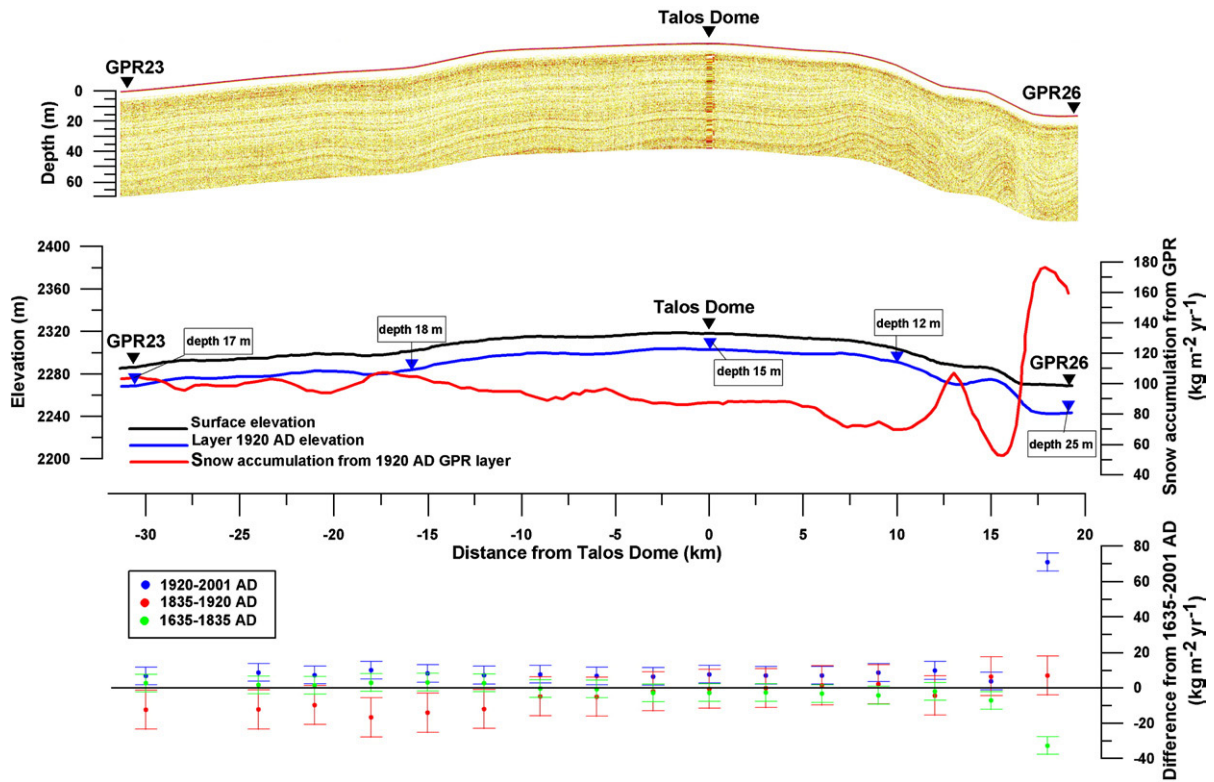


Fig. 4. Talos Dome snow radar profile from GPR23 to GPR26 (position is shown in Fig. 3). Elevation, S1 snow radar elevation profile (numbers indicate the depth of the layer) and the 81 yr average of snow accumulation inferred from GPR are shown. Difference in accumulation inferred from GPR for three different periods are shown with error bars.

prevailing wind directions have a considerable impact on the spatial distribution of snow on short (tens of meters) and medium (kilometer) spatial scales (Frezzotti et al., 2004b, 2005, 2007). Changes in wind conditions could determine a decrease/increase in snow accumulation in upwind/downwind areas. Accumulation records from stakes and firn cores at the TD summit show increases over the past 200 yr; the increase has been more pronounced since the 1960s atomic bomb markers as compared to the previous period from Tambora onward (1816–1965 AD). However, since the 1990s a decrease in accumulation (about 10%) has been observed as compared to the 20th century average, as computed from stake measurements (Frezzotti et al., 2007). Snow accumulation measurements (4 stake farms and 5 firn cores) taken along the 500 km transect crossing TD show no significant increases in accumulation over the last two centuries (Frezzotti et al., 2007). In a previous paper, Stenni et al. (2002), who based their findings on a single firn core, reported a decrease in accumulation during a part of the LIA (1643–1902 AD), followed by an increment in accumulation of about 11% during the 20th century (1902–1996 AD).

3.1.2. Dome C

Elevation contour lines (Fig. 6) show that the most prominent characteristic of the DC surface is its elliptical shape, with the minor axis (NW–SE) being about 70% shorter than the major (SW–NE) axis (Rémy and Tabacco, 2000). The elongation direction of the dome is parallel to the prevalent SW–NE wind direction (Frezzotti et al., 2005). Comparison of snow accumulation of two cores (site A17 at DC), drilled tens of meters apart, reveals an 11% difference in accumulation for the tritium/ β marker horizons. Comparison of snow accumulation data derived from 16 firn core records (using atomic bomb and Tambora markers) and from GPR isochrones (using EPICA depth–age function) at DC shows good agreement within the experimental error (Fig. 2). The difference of snow accumulation values between cores and snow radar data reflects temporal and spatial differences among sample areas, snow accumulation variability at the core scale and the increase in snow accumulation at DC since 1960 (Frezzotti et al., 2005). The depth of GPR layers increases from South to North (up to 1.5 m in 50 km; Fig. 7). The deepening of layers and the related increase in accumulation is more pronounced at the Concordia

Station to the North. The depth increase is equivalent to a South–North increase in snow accumulation rate of about $0.02 \pm 0.01 \text{ kg m}^{-2} \text{ yr}^{-1}$ per km from the South to Concordia Station and about $0.08 \pm 0.01 \text{ kg m}^{-2} \text{ yr}^{-1}$ per km from the Concordia Station to the North. The snow accumulation map and profile (Figs. 6 and 7) clearly show this pattern, with a marked increase in accumulation in the northern part of DC. This accumulation pattern was poorly defined by core data and snow radar L1 (dated to 1921 ± 3 AD) due to a “relatively larger error” (from ± 1.5 to $\pm 3.4 \text{ kg m}^{-2} \text{ yr}^{-1}$), with respect to the local spatial variability in snow accumulation (about $\pm 0.9 \text{ kg m}^{-2} \text{ yr}^{-1}$, 3%) relative to the accumulation gradient (about $3 \text{ kg m}^{-2} \text{ yr}^{-1}$ per 50 km) and the observation time span (Fig. 2). This spatial snow accumulation gradient is present in all layers but is more observable in the deepest layers.

The following observations, in addition to the local accumulation pattern discussed above, indicate that DC is a key area that marks the change in accumulation distribution, with a decrease in the accumulation gradient to the South and East:

- (1) based on the Tambora marker (Legrand and Delmas, 1987; Frezzotti et al., 2005), the accumulation gradient is $0.01 \text{ kg m}^{-2} \text{ yr}^{-1} \text{ km}^{-1}$ between Vostok and DC (650 km) and $0.08 \text{ kg m}^{-2} \text{ yr}^{-1} \text{ km}^{-1}$ between DC and old Dome C (55 km NE of DC, Fig. 1);
- (2) SW–NE deep ice-penetrating radar transect (800 km long) centred at DC (Siegert, 2003) shows a relatively abrupt increase in the accumulation rate just NE of DC;
- (3) present regional accumulation data from West (Young et al., 1982) to East (Frezzotti et al., 2004b) show a decrease in accumulation in the eastern part of DC; and
- (4) $\delta^{18}\text{O}$ values for the sites East of DC along the DC–Terra Nova Bay transect are more negative than those for DC and the West and North sides, probably due to isotope depletion in precipitation, which is induced by an orographic “shadowing” effect in the eastern DC area (Magand et al., 2004).

Using nssSO_4^{2-} volcanic spikes (Castellano et al., 2005) from the last 500 yr, an analysis of snow accumulation in the EPICA EDC96 core shows that accumulation was lower ($< 25 \text{ kg m}^{-2} \text{ yr}^{-1}$) during the Kuwae–Tambora period (1460–1816 AD) than from Tambora to the present ($> 26 \text{ kg m}^{-2} \text{ yr}^{-1}$). Frezzotti et al. (2005) used a stake network within 25 km of Concordia Station ($39 \text{ kg m}^{-2} \text{ yr}^{-1}$; 1996–1999 AD) and atomic bomb markers for 18 firn cores (28.3 kg m^{-2}

yr^{-1} 1965–2000 AD) and observed a recent temporal increase in snow accumulation compared to the Tambora period ($25.3 \text{ kg m}^{-2} \text{ yr}^{-1}$ 1816–1998 AD). A stake farm network that was established in 2004 close to Concordia and re-measured seasonally, within the framework of the Station observatory (<http://www-igge.obs.ujf-grenoble.fr/~christo/glacioclim/samba>), confirms the significant increase in the observed accumulation ($\sim 32 \text{ kg m}^{-2} \text{ yr}^{-1}$). Moreover, temporal variability of deuterium excess (proxy of oceanic moisture source conditions) at the old DC site and EPICA EDC96 cores (Lorius et al., 1979; Stenni et al., 2001) and sodium at the EDC96 core (proxy of marine aerosol; Röthlisberger et al., 2000) shows an atmospheric moisture source variation between 1580–1710 AD and 1710 AD to the present (Fig. 8).

Backward air parcel trajectories reveal that the resulting snowfall trajectories at DC come from the North (Reijmer et al., 2002). The present-day and palaeo-accumulation is driven by the direction of snowfall and its interaction with “orography”. The suggested changes in the eccentricity of the polar vortex during past glacial

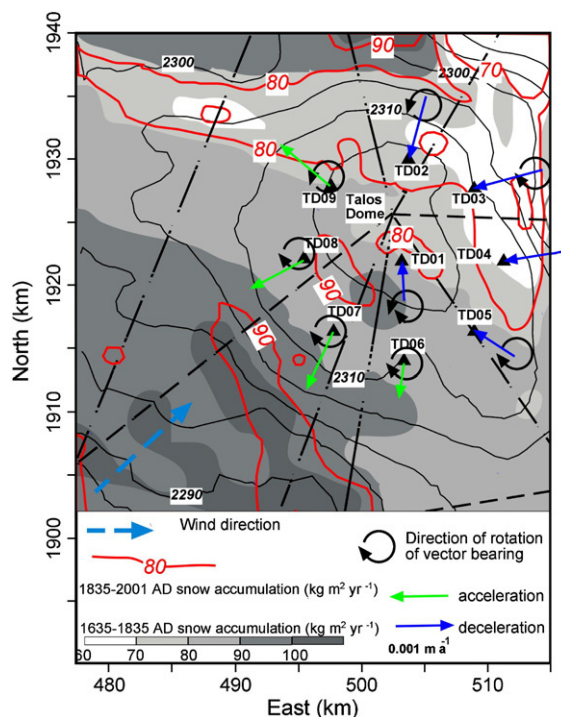


Fig. 5. Palaeo-accumulation (S3 less S2: 1635–1835 AD grey scale) and present accumulation (surface less S2: 1835–2001 AD red contour) maps based on snow radar data. Green, blue and black arrows indicate vector of ice velocity acceleration–deceleration and direction of rotation bearing. Contour lines of surface topography have a 5 m interval. Snow radar profiles (dotted line) and prevalent wind direction (cyan arrow) are shown.

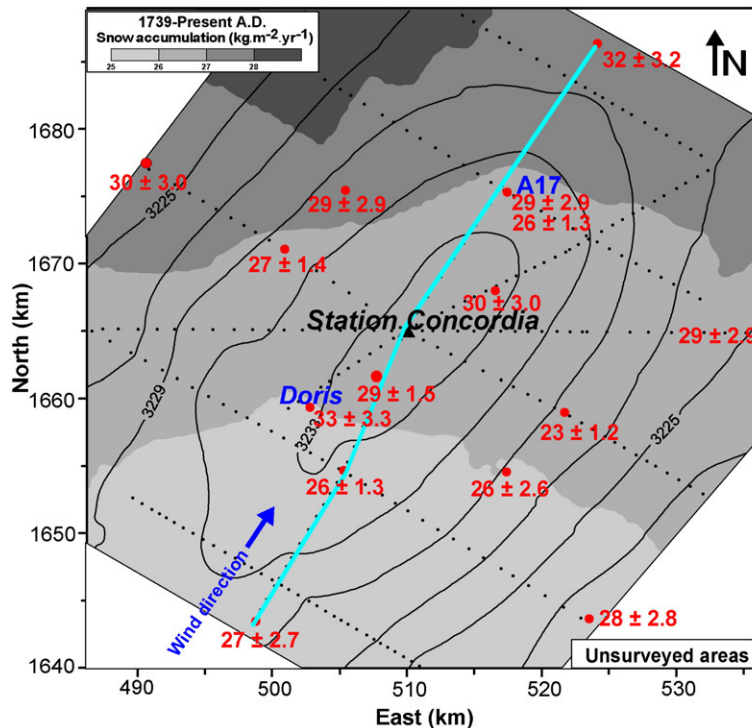


Fig. 6. Dome C snow accumulation map ($\text{kg m}^{-2} \text{yr}^{-1}$) based on snow radar data (L5: 1710–2000 AD) and snow accumulation values (in red) derived from firn core analysis (tritium/ β marker: 1965–2000 AD). Contour lines of surface topography are placed at 2 m intervals. The dashed line indicates snow radar profiles. The cyan line indicates the elevation and snow radar profile of Fig. 7.

periods (Delmonte et al., 2004; Udisti et al., 2004), coupled with a change in the atmospheric pathway of snowfall (from N to NE and/or E), may have influenced the distribution of accumulation and shape/position of the dome. A reconstruction of the ice sheet accumulation rate at Ridge B shows that the western flank of the ice divide experiences markedly more accumulation than the East; moreover, records for the last 124 kyr show temporal and spatial variability around the Ridge B ice divide (Ley-singer Vieli et al., 2004).

An analysis of GPR-based palaeo-accumulation distribution data (Figs. 7, 8 and 9) reveals a general pattern of increase and decrease in accumulation rates, with the lowest value falling in the period 1602–1739 AD and the highest from 1739 to 1869 AD. Based on palaeo-accumulation distribution data for the southern and eastern areas of DC, the accumulation distribution does not appear to have changed significantly between the past and present. In the northern part, by contrast, the palaeo-accumulation distribution pattern shows a counter-clockwise rotation from East to West, with an increase in asymmetry between the accumulation pattern and the morphology shape of the dome (Fig. 9). Based on observations at different sites in East Antarctica (South Pole, DC, TC, Vostok etc.), an increase in accumulation

has occurred over the last two centuries and during the period between the 1960s and 1990s, with cyclic variation at the decadal scale. However, no significant increase has been observed since the 1990s at several sites in East Antarctica (Frezzotti et al., 2005, 2007 and reference therein). Snowfall accumulation across the continent has been investigated since the 1950s by combining model simulations and observations primarily from firn cores, and the research suggests that there has been no substantial increase but rather a slight downturn in accumulation in the past decade (Monaghan et al., 2006).

The significant increase in snow accumulation observed at DC since the 1990s, but not in other East Antarctica sites, could be correlated with oddly increased precipitation at the sites. However, a different snowfall trajectory could likewise have resulted in an increase of accumulation, given the different spatial distribution at the dome site.

3.2. Ice velocity change

3.2.1. Talos Dome

At TD, the highest horizontal velocities were recorded for the “steeper” S–SW and E–NE slopes, whereas the lowest horizontal velocities were recorded

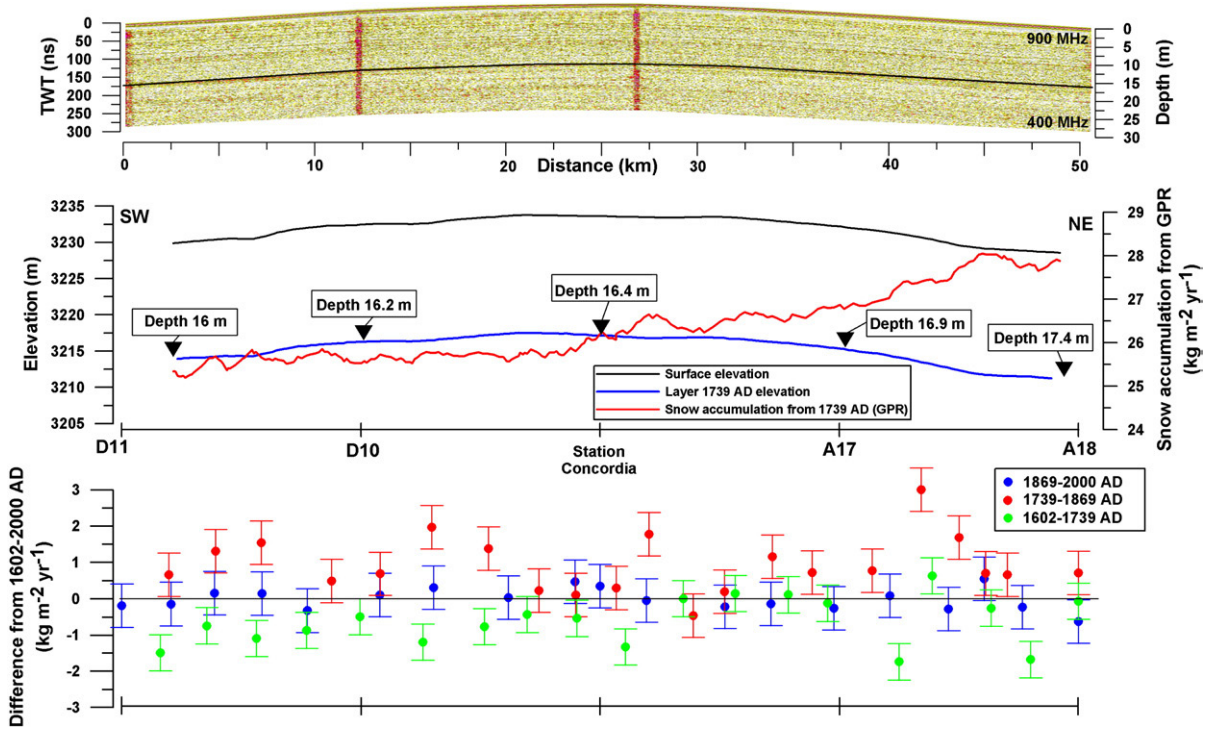


Fig. 7. Dome C snow radar profile from SW to NE along the major axis of Dome C (position is reported in Fig. 6). Elevation, L5 snow radar elevation profile (numbers indicate the depth of the layer) and the 290 yr average of snow accumulation profile are inferred from GPR. Differences of accumulation inferred from GPR for three different periods are shown with error bars.

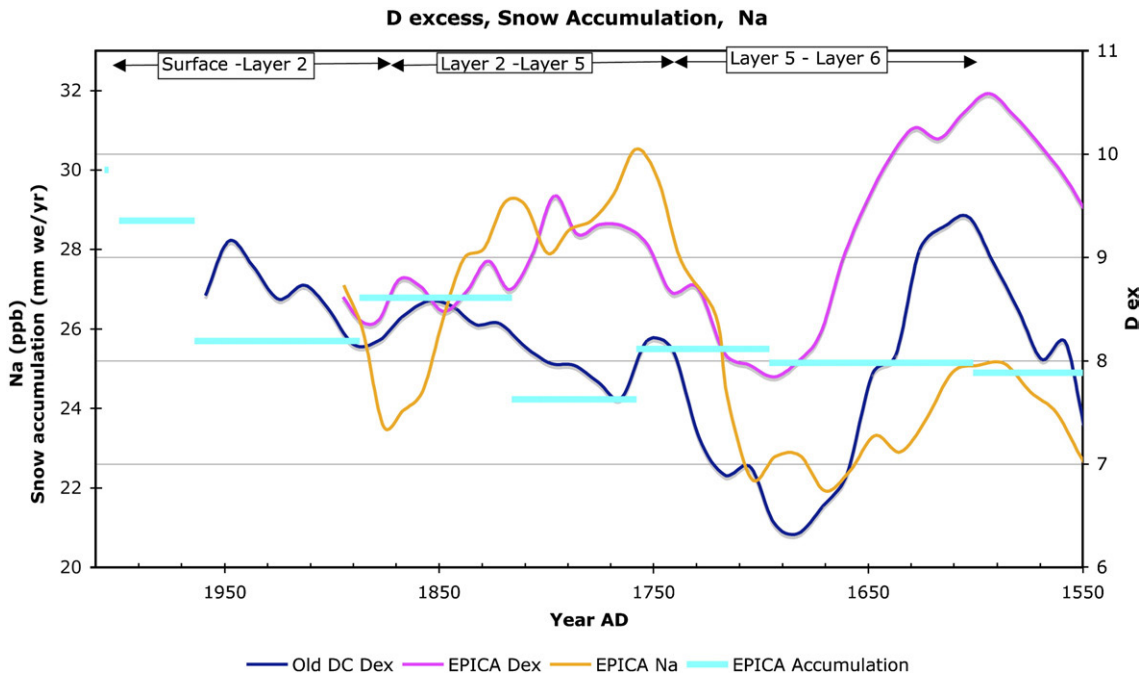


Fig. 8. Temporal variability (5 data average) of D excess (%) and sodium at EPICA EDC96 (from IGBP PAGES/World Data Center for Paleoclimatology Data Contribution Series #2005-048; Röthlisberger et al., 2000; Stenni et al., 2001; Stenni pers. com. 2005), D excess of old Dome C (Lorius et al., 1979) and EPICA EDC96 snow accumulation (1550–1998 AD) from both nssSO_4^{2-} volcanic spikes (Castellano et al., 2005) and stake farms (1996–2005 AD).

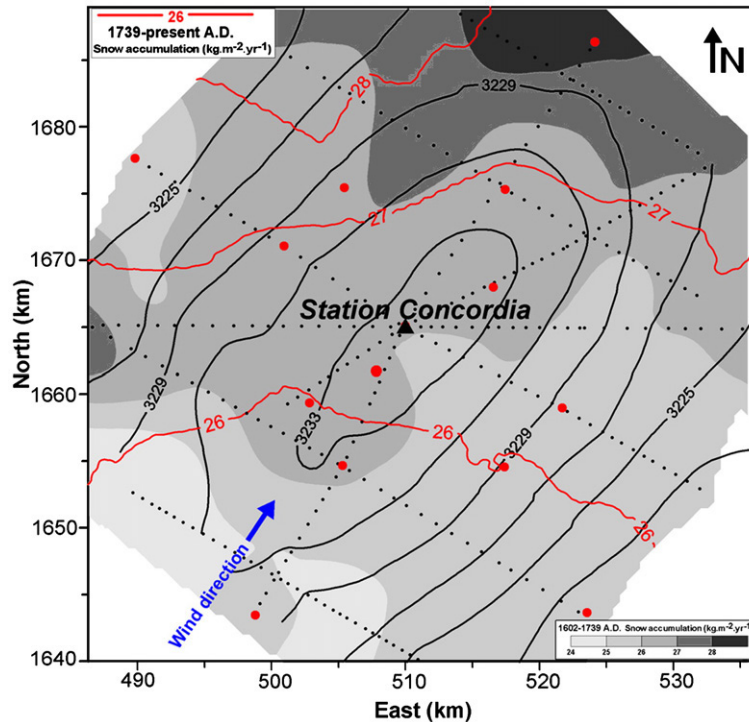


Fig. 9. Dome C snow palaeo-accumulation map based on snow radar data (L6 less L5: 1602–1739 AD). Red contour lines of accumulation map from present back to 1739 AD (Fig. 7). Contour lines of surface topography are placed at 2 m intervals. The dashed line indicates snow radar profiles.

close to the dome summit and along the SE ice divide (Frezzotti et al., 2004a). Data (Table 1, Fig. 5) reveals deceleration from 5 ± 3 to 2 ± 3 mm yr^{-2} in the sector from North to SE (from TD01 to TD05) and acceleration from 1 ± 3 to 4 ± 3 mm yr^{-2} in the sector from NW to South (from TD06 to TD09). Although velocity changes below 3 mm yr^{-2} fall within the margin of error due to measurement uncertainty, the geographical distribution of all acceleration/deceleration measurements are coherent at each site and are higher than the level of uncertainty in 5 out of 9 measurements (Table 1). The bearing rotates counter-clockwise in the North and NW portions and clockwise in other sectors. The snow radar profile reveals an approximately 10% increase in accumulation in the SW part. Due to the very low slope gradient, it is difficult to evaluate changes in slope.

At the dome, where the surface slopes vary little, the ice dynamics are very low and appear to be a complex function of slope, ice thickness/bedrock conditions and the snow accumulation rate distribution. It is difficult to determine the factors influencing the absolute position of the dome because plate tectonics determines values that are similar to or higher than the dome migration ascribable to glacio-climatological factors. In order to

determine absolute displacement through repeated surveys, the effects of the tectonic motion of the Antarctic plate must be modelled and corrected. Our analysis takes into account the tectonic displacement of the Antarctic plate extracted from the global model Nuvel 1A-NNR 1991 (Argus and Gordon, 1991; Altamini et al., 2002) and verified within Victoria Land through repeated GPS measurements of the Victoria Land deformation network (VLNDEF). The main observable effect is induced by the rotational–translational motion of the continent as a whole (Dietrich and Rulke, 2002; Negusini et al., 2005), with the approximate motion of the continent that was extrapolated at TD01 being $\sim 15 \text{ mm yr}^{-1}$ with an azimuth of 141° . Acceleration–deceleration at TD occurs in a SW direction, whereas the tectonic movement of the continent is at 90° in a SE direction.

3.2.2. Dome C

GPS measurements indicate that poles closest to the DC summit move up to a few mm yr^{-1} , while poles located 25 km from the summit move up to 211 mm yr^{-1} (Vittuari et al., 2004). Two years of continuous GPS measurements at the Concordia Station-EPICA site allow

the determination of absolute velocity to be 10.9 ± 0.6 mm yr^{-1} with a direction of 302° . The absolute movement of DC is within the instrumental error of about ± 7 mm yr^{-1} , and no absolute horizontal movement of the dome could be detected on the basis of two measurements made 3 yr apart (Vittuari et al., 2004). Within 25 km of DC, the ice thickness and bedrock topography oscillate with amplitudes of up to ± 400 m, with greater thicknesses observed to the North and lower thicknesses to the South (Forieri et al., 2003). Balance velocity calculations based on the system proposed by Legresy et al. (2000) are in agreement with ice velocity measurements and detection limits. The greater thickness in the northern DC area compensates the relatively higher accumulation in balance velocity. The combination of a low accumulation gradient (0.02 – 0.08 kg m^{-2} yr^{-1} per km) and slope (less than 0.5 m per km) and relatively large variations in ice thickness (± 400 m) hinders the detection of ice velocity (± 7 mm yr^{-1}) or strain rate (about 10^{-5} yr^{-1}) differences using GPS or remote sensing surveys carried out 3 yr apart within 25 km of the summit. In the near future, repeat measurements of the DC strain network will allow the detection of possible changes in ice velocity in the northern sector of the dome, but only a fourth repetition taking place more than 15 yr after the first measurements will allow the detection of a possible velocity change.

4. Conclusions

The accumulation map obtained from snow radar data reveals a significant spatial variability in the snow accumulation rate at Talos Dome and Dome C. Accumulation distributions are not symmetrical in relation to dome morphology, and the accumulation distribution pattern has changed over the last few centuries. At Talos Dome the accumulation value for the period 1835–1920 AD is significantly lower than the values for the previous (1635–1835 AD) and subsequent (1920–2001 AD) periods in the SW part, whereas in the NE, accumulation in the same period is more similar to that observed for the other two periods. The palaeo-accumulation distribution at Talos Dome shows a decrease in the accumulation gradient along the wind direction, which could be due to changes in the wind-driven accumulation process. Repeated GPS measurements made at Talos Dome have highlighted changes in ice velocity, with a decrease in velocity in the NE portion and an increase in the order of mm yr^{-2} in the SW portion. As a result of the changed accumulation conditions, the Talos Dome summit has probably migrated to SE in the last few centuries. Findings in the northern part of Dome C indicate that the

accumulation distribution has undergone a counter-clockwise rotation in the last 260 yr (from 1739 AD to present) relative to the pattern of the previous 130 yr (from 1602 to 1739 AD). At both domes, we observed a change in the distribution pattern at the century scale and a significant increase in accumulation at Dome C since the 1990s, which could be correlated with changes in snow accumulation patterns that reflect a change in snowfall trajectory. The difference between present and past accumulation reveals that the dynamics of the domes change from the decadal and century scales. Snow accumulation distribution mechanisms are different at the two domes: a wind-driven snow accumulation process operates at Talos Dome, whereas snowfall trajectory is the main factor at Dome C.

The spatial variability at km scale of snow accumulation is very important on the Antarctic Ice Sheet and also at the dome site and is of the same order of magnitude or greater than temporal variability at the multi-decade/secular scale. Moreover, past changes in snow accumulation distributions have consequences on the flow direction of ice and dome–ice divide morphology and relationships (e.g., presence/absence of saddles connecting the domes to the ice divides). The study of the position and environmental characteristics of ice divides under the present climatic conditions will help determine past variations in ice divides and dome positions.

The ongoing change of a dome–ice divide cannot be detected through annual-scale measurements; rather, repeated measurements spanning several decades are required.

Acknowledgements

Research was carried out in the framework of the Project on Glaciology of the PNRA-MIUR and was financially supported by the PNRA Consortium through collaboration with ENEA Roma. This paper is a French–Italian contribution to the ITASE and Concordia Station projects and the EPICA and TALDICE projects. EPICA is a joint ESF (European Science Foundation)/EU scientific programme funded by the European Commission and by national contributions from Belgium, Denmark, France, Germany, Italy, the Netherlands, Norway, Sweden, Switzerland and the United Kingdom. The present research was made possible by the joint French–Italian Concordia Program, which established and runs the permanent station Concordia at Dome C. Talos Dome Ice core Project (TALDICE), a joint European programme, is funded by national contributions from Italy, France, Germany,

Switzerland and the United Kingdom. Main logistic support was provided by PNRA. This is EPICA publication no. 185 and TALDICE publication no 1.

References

- Altamini, Z., Sillard, P., Boucher, C., 2002. ITRF2000 a new release of the International Terrestrial Reference Frame for Earth Science Applications, *J. Geophys. Res.*, 107 (B10), 2214, 2-19. [10.1029/2001JB00056](https://doi.org/10.1029/2001JB00056).
- Anandkrishnan, S., Alley, R.B., Waddington, E.D., 1994. Sensitivity of the ice-divide position in Greenland to climate change. *Geophys. Res. Lett.* 21 (6), 441–444.
- Argus, D., Gordon, R., 1991. No-Net Rotational model of current plate velocities incorporating plate motion model NUVEL-1. *Geophys. Res. Lett.* 18 (11), 2039–2042.
- Brisset, L., Remy, F., 1996. Antarctica surface topography and kilometric scale features derived from ERS-1 satellite altimeter. *Ann. Glaciol.* 23, 374–381.
- Capra, A., Cefalo, R., Gandolfi, S., Manzoni, G., Tabacco, I.E., Vittuari, L., 2000. Surface topography of Dome Concordia (Antarctica) from kinematic interferential GPS and bedrock topography. *Ann. Glaciol.* 30, 42–46.
- Castellano, E., Becagli, S., Hansson, M., Hutterli, M., Petit, J.R., Rampino, M.R., Severi, M., Steffensen, J.P., Traversi, R., Udisti, R., 2005. Holocene volcanic history recorded in the sulphate stratigraphy of the EPICA-EDC96 ice core (Dome C, Antarctica). *J. Geophys. Res.* 110 (D06114). [doi:10.1029/2004JD005259](https://doi.org/10.1029/2004JD005259).
- Cefalo, R., Tabacco, I.E., and Manzoni, G., 1996. Processing of kinematic GPS trajectories at Dome C (Antarctica) and altimetry interpretations, In Unguendoli, M., ed. Reports on Surveying and Geodesy, Bologna, DISTART ed. Nautilus, Università degli Studi di Bologna, 204–222.
- Delmonte, B., Petit, J.R., Andersen, K.K., Basile-Doelsh, I., Maggi, V., Lipenkov, V.Y., 2004. Dust size evidence for opposite regional atmospheric circulation changes over East Antarctica during the last climatic transition. *Clim. Dyn.* 23. [doi:10.1007/s00382-004-0450-9](https://doi.org/10.1007/s00382-004-0450-9).
- Dietrich, R., Rulke, A., 2002. Present status of the SCAR GPS database. Proceedings of the SCAR Antarctic Geodesy Symposium AGS02 on Regional Geodetic Networks, Wellington, New Zealand.
- Eisen, O., Nixdorf, U., Wilhelms, F., Miller, H., 2004. Age estimates of isochronous reflection horizons by combining ice core survey, and synthetic radar data. *J. Geophys. Res.* 109 (B4106). [doi:10.1029/2003JB002858](https://doi.org/10.1029/2003JB002858).
- EPICA, community members, 2004. Eight glacial cycles from an Antarctic ice core. *Nature* 429, 623–628.
- Frieri, A., Tabacco, I.E., Della Vedova, A., Zirizzotti, A., Bianchi, C., De Michelis, P., Passerini, A., 2003. A new bedrock map of the Dome C area. *Terra Antarctica Report* 8, 169–170.
- Frezzotti, M., Gandolfi, S., Urbini, S., 2002. Snow megadunes in Antarctica: sedimentary structure and genesis. *J. Geophys. Res.* 107 (D18) 4344. [10.1029/2001JD000673](https://doi.org/10.1029/2001JD000673) 1–12.
- Frezzotti, M., Bitelli, G., de Michelis, P., Deponti, A., Frieri, A., Gandolfi, S., Maggi, V., Mancini, F., Remy, F., Tabacco, I.E., Urbini, S., Vittuari, L., Zirizzotti, A., 2004a. Geophysical survey at Talos Dôme (East Antarctica): the search for a new deep-drilling site. *Ann. Glaciol.* 39, 423–432.
- Frezzotti, M., Pourchet, M., Flora, O., Gandolfi, S., Gay, M., Urbini, S., Vincent, C., Becagli, S., Gragnani, R., Proposito, M., Severi, M., Traversi, R., Udisti, R., Fily, M., 2004b. New estimations of precipitation and surface sublimation in East Antarctica from snow accumulation measurements. *Clim. Dyn.* 23(7–8), 803–813. [doi:10.1007/s00382-004-0462-5](https://doi.org/10.1007/s00382-004-0462-5).
- Frezzotti, M., Pourchet, M., Flora, O., Gandolfi, S., Gay, M., Urbini, S., Vincent, C., Becagli, S., Gragnani, R., Proposito, M., Severi, M., Traversi, R., Udisti, R., Fily, M., 2005. Spatial and temporal variability of snow accumulation in East Antarctica from traverse data. *J. Glaciol.* 51 (207), 113–124.
- Frezzotti, M., Urbini, S., Proposito, M., Scarchilli, C., Gandolfi, S., 2007. Spatial and temporal variability of surface mass balance near Talos Dome, East Antarctica. *J. Geophys. Res.* 112 (F02032). [doi:10.1029/2006JF000638](https://doi.org/10.1029/2006JF000638).
- Hindmarsh, R.C.A., 1996. Stochastic perturbation of divide position. *Ann. Glaciol.* 23, 94–104.
- Legrand, M., Delmas, R.J., 1987. A 220-year continuous record of volcanic H₂SO₄ in the Antarctic ice sheet. *Nature* 327, 671–676.
- Legresy, B., Rignot, E., Tabacco, I.E., 2000. Constraining ice dynamics at Dome C, Antarctica, using remotely sensed measurements. *Geophys. Res. Lett.* 27 (21), 3493–3496.
- Leysinger Vieli, G.J.M.-C., Siegert, M.J., Payne, A.J., 2004. Reconstructing ice-sheet accumulation rates at ridge B, East Antarctica. *Ann. Glaciol.* 39, 326–330.
- Lorius, C., Merlivat, L., Jouzel, J., Pourchet, M., 1979. A 30,000 yr isotope climatic record from Antarctic ice. *Nature* 280, 644–648.
- Magand, O., Frezzotti, M., Pourchet, M., Stenni, B., Genoni, L., Fily, M., 2004. Climate variability along latitudinal and longitudinal transects in East Antarctica. *Ann. Glaciol.* 39, 351–358.
- Monaghan, A.J., Bromwich, D.H., Fogt, R.L., Wang, S.H., Mayewski, P.A., Dixon, D.A., Ekaykin, A., Frezzotti, M., Goodwin, I., Isaksson, E., Kaspari, S.D., Morgan, V.I., Oerter, H., Van Ommen, T., Van der Veen, C.J., Wen, J., 2006. Insignificant change in Antarctic snowfall since the International Geophysical Year. *Science* 313, 827–831.
- Negusini, M., Mancini, F., Gandolfi, S., Capra, A., 2005. Terra Nova Bay GPS permanent station (Antarctica): data quality and first attempt in the evaluation of regional displacement. *J. Geodyn.* 39, 81–90.
- Nereson, N.A., Raymond, C.F., Waddington, E.D., Jacobel, R.W., 1998. Migration of the Siple Dome ice divide, West Antarctica. *J. Glaciol.* 44 (148), 643–652.
- Reijmer, C.H., van den Broeke, M.R., Scheele, M.P., 2002. Air parcel trajectories and snowfall related to five deep drilling locations in Antarctica based on the ERA-15 Dataset. *J. Climate* 15, 1957–1968.
- Remy, F., Tabacco, I.E., 2000. Bedrock features and ice flow near the EPICA ice core site (Dome C, Antarctica). *Geophys. Res. Lett.* 27, 405–408.
- Ritz, C., Rommelaere, V., Dumas, C., 2001. Modelling the evolution of Antarctic ice sheet over the last 420,000 years: implications for the altitude changes in the Vostok region. *J. Geophys. Res.* 106, 31,943–31,964.
- Richardson, C., Aarholt, E., Hamran, S.-E., Holmlund, P., Isaksson, E., 1997. Spatial snow distribution of snow in western Dronning Maud Land, East Antarctica, mapped by a ground based snow radar. *J. Geophys. Res.* 102 (B9), 20,343–20,353.
- Röthlisberger, R., Hutterli, M.A., Sommer, S., Wolff, E.W., Mulvaney, R., 2000. Factors controlling nitrate in ice cores: evidence from the Dome C deep ice core. *J. Geophys. Res.* 105 (D16), 20,565–20,572.
- Siegert, M.J., 2003. Glacial–interglacial variations in central East Antarctica ice accumulation rates. *Quat. Sci. Rev.* 22, 741–750.
- Spikes, V.B., Arcone, S., Hamilton, G., Mayewski, P., Dixon, D., Kaspari, S., 2004. Spatial and temporal variability in West Antarctic snow accumulation rates. *Ann. Glaciol.* 39, 238–244.

- Stenni, B., Masson-Delmotte, V., Johnsen, S., Jouzel, J., Longinelli, A., Monnin, E., Röthlisberger, R., Selmo, E., 2001. An oceanic cold reversal during the last deglaciation. *Science* 293, 2074–2077.
- Stenni, B., Proposito, M., Gragnani, R., Flora, O., Jouzel, J., Falourd, S., Frezzotti, M., 2002. Eight centuries of volcanic signal and climate change at Talos Dome (East Antarctica). *J. Geophys. Res.* D9 (107). doi:10.1029/2000JD000317, 1–14.
- Udisti, R., Becagli, S., Castellano, E., Delmonte, B., Jouzel, J., Petit, J.R., Schwander, J., Stenni, B., Wolff, E., 2004. Stratigraphic correlations between the European Project for Ice Coring in Antarctica (EPICA) Dome C and Vostok ice cores showing the relative variations of snow accumulation over the past 45 kyr. *J. Geophys. Res.* 109 (D8101). doi:10.1029/2003JD004180.
- Udisti, R., Becagli, S., Castellano, E., Mulvaney, R., Schwander, J., Torcini, S., Wolff, E., 2000. Holocene electrical and chemical measurements from the EPICA-Dome C ice core. *Ann. Glaciol.* 30, 20–26.
- Vaughan, D.G., Corr, H.J.F., Doake, C.S.M., Waddington, E.D., 1999. Distortion of isochronous layers in ice revealed by ground-penetrating radar. *Nature* 398 (6725), 323–326.
- Vincent, C., Pourchet, M., 2000. Geodetic measurements and accumulation rate at Dome Concordia, December 1999 and January 2000. Grenoble, Laboratoire de Glaciologie et Géophysique de l'Environnement. Institut Français pour la Recherche et la Technologie Polaire and for Ente per le Nuove Tecnologie l'Energia e l'Ambiente, (Technical Report.). 15 pp.
- Vittuari, L., Vincent, C., Frezzotti, M., Mancini, F., Gandolfi, S., Bitelli, G., Capra, A., 2004. Space geodesy as a tool for measuring ice surface velocity at the Dome C site and between Terra Nova Bay and Dome C (East Antarctica). *Ann. Glaciol.* 39, 402–408.
- Young, N.W., Pourchet, M., Kotlyakov, V.M., Korolev, P.A., Dyugerov, M.B., 1982. Accumulation distribution in the IAGP area, Antarctica: 90°E–150°E. *Ann. Glaciol.* 3, 333–338.